

Optical and mechanical design considerations in the construction of a 24" phase shifting interferometer

Joe Lamb, James Semrad, James Wyant, Chiayu Ai,
Robert Knowlden, Erik Novak, John Downie, Robert Wolfe

WYKO Corporation
2650 E. Elvira Rd., Tucson, AZ, 85706, USA

ABSTRACT

WYKO Corporation is currently designing and manufacturing specialized phase shifting interferometers to aid in the qualification of large optics for the U.S. N.I.F. program. The interferometers will be used to qualify homogeneity of raw material and provide in-process inspection information and final inspection qualification data. The 24" systems will be the largest commercially available Fizeau phase shifting interferometers ever manufactured. Systems will be produced using traditional CCD cameras as well as a megapixel CCD camera for applications requiring higher lateral resolution. Mechanical and optical design considerations include vibration and distortion control of critical optical elements, polarization control of the laser source, imaging system design, and optical transfer function optimization. We also address effects in the test cavity arising from measuring transmitted and reflected wavefronts of optics mounted at Brewster's angle.

Keywords: interferometer, optical testing, phase shifting

1. INTRODUCTION

Construction of the U.S. National Ignition Facility¹ will require fabricating more than 8000 large planar optics having apertures of approximately 40 x 40 cm. Some of these elements such as the laser amplifier slabs and glass polarizer plates will be used at Brewster's angle. Therefore, these optics will be rectangular and approximately 73 x 40 cm in size. These optics must be measured both at full aperture and at reduced aperture to provide the higher resolution measurements necessary to detect mid-spatial frequency errors in the optics. Further, the requirement for high spatial frequency sampling and high wavefront accuracy require a phase shifting interferometer. To accurately measure the entire 40 x 40 cm aperture in a single measurement the interferometer must have at least a 57 cm aperture. Since no commercial interferometers exist at this size or larger, WYKO has designed, and is currently building, the first instrument capable of meeting the size, accuracy, and resolution goals of the N.I.F. test plan. Below, we describe the requirements for the interferometer and discuss the more challenging aspects of both the mechanical and optical design.

2. MEASUREMENT CHARACTERISTICS

Table 1 summarizes the characteristics of the interferometer. A more detailed discussion follows.

2.1 Field of view and spatial resolution

The interferometer has two modes of operation: a wide field mode that covers a 43 cm square, and a narrow field mode that gives more detailed data over a 10 cm square subsection of an object. With a high-resolution camera (1000 x 1000 pixels), the pixel spacings as projected onto the object are 0.44 mm and 0.10 mm for the wide and narrow field modes.

2.2 Instrument transfer function

The system instrument transfer function (ITF) was optimized to ensure the measurements were accurate at the target resolution. Define ITF as:

$$ITF = \sqrt{\frac{PSD_{meas.}}{PSD_{true}}}$$

(1)

The system ITF was optimized in a prototype optical system using several proprietary techniques and compared to current WYKO and other commercial interferometers. At the specified resolutions for the two fields of view, ITF is better than 70%.

2.3 Measurement angle and polarization

Plate polarizers and laser amplifier slabs are to be measured at their angle of use (Brewster's angle; Figure 1). This ensures measurement of any angle-sensitive phenomena (e.g., birefringence) at the strength at which they would be present in use. Taking data at Brewster's angle also allows testing of the rectangular plates at full aperture in a single measurement with a 61 cm interferometer aperture. An 89 cm (35") aperture system would be needed to measure the plates at normal incidence. The 24" (61 cm) system is much less expensive than an 89 cm. system.

The parts to be tested in transmission at Brewster's angle will not be wedged, so the use of TM (transverse magnetic field) polarized light eliminates their surface reflections and the associated spurious fringes. Measurements in reflection of the plates' surfaces will also be done near Brewster's angle (Figure 2), but using TE (transverse electric field) light to *maximize* the reflectance.

3. TILTED PLATE EFFECTS

There is a drawback to testing a tilted plate; the gap between the RF (return flat) and the plate varies by approximately 61 cm. The gap produces errors due to beam walk-off (described by geometric optics) and diffraction effects (described by the Fresnel theory).

3.1 Beam walk-off

If the beam is not accurately perpendicular to the RF, the gap between the RF and the test piece will cause the beam in the transmission test to return through a slightly different area of the piece on the beam's second pass (Figure 3). If this walk-off is less than one-quarter pixel, its effects will not be readily visible. We have specified the ray slope error from *all sources* (including alignment of the beam to the RF, and aberrations in the collimator lens) to be less than 5 arc seconds (25 μ rad). With a round-trip distance of 160 cm, the walk-off is 0.04 mm. This is less than 0.1 pixel for the wide FOV (field of view) mode, but it is approximately 0.4 pixel for the narrow FOV mode. We will see below that a 40 cm round-trip distance (20 cm gap) will be required in the narrow FOV mode to avoid diffraction effects.

3.2 Diffraction effects

Diffraction results from the free-space propagation of the beams in the interferometer, and is a consequence of having a gap between the test piece and the RF. Consider a weak sinusoidal phase grating with complex transmittance:

$$\tau(x) = e^{j\alpha \cos(\frac{2\pi x}{\Lambda} + \phi_0)} \approx 1 + j\alpha \cos(\frac{2\pi x}{\Lambda} + \phi_0) \quad (2)$$

where α is the amplitude of the grating ($0 < \alpha \ll 1$), Λ is the grating's period, and ϕ_0 is a phase constant. (For the purposes of this discussion, we ignore the tilt of the test piece, and assume the piece to be at a fixed distance from the RF.) The transfer function for Fresnel diffraction (cf. Goodman²) is:

$$H(v) = e^{\frac{j2\pi z}{\lambda}} e^{-j\pi\lambda z v^2} \quad (3)$$

where z is the total propagation distance between the object on the first pass and the second (twice the gap between the object and the RF), v is spatial frequency, and λ is the wavelength of the light. For a periodic structure of period Λ , the Talbot self-imaging distance² is:

$$z_T = \frac{2\Lambda^2}{\lambda} \quad (4)$$

At half the Talbot distance, the image of the phase grating undergoes a phase reversal (with respect to the zero-frequency component), and *cancels* the grating on the second pass. At one quarter of the Talbot distance, the phase grating will appear as an *amplitude* grating. In practice, the interferometer would be focused at the RF, so the weak grating in double-pass may be approximated as having a transmittance:

$$\tau_D(x) \approx 1 + 2j\alpha \cos\left(\frac{\pi\lambda d}{\Lambda^2}\right) \cos\left(\frac{2\pi x}{\Lambda} + \phi_0\right) \quad (5)$$

where d is the spacing between the grating and the RF (above, $z = 2d$), and the registration of the two passes is perfect (zero walk-off). Define the acceptable spacing to be:

$$d \leq \frac{\Lambda^2}{8\lambda} \quad (6)$$

for an apparent grating depth greater than 0.92 of its true value. In the wide field mode (above), $\Lambda = 4$ mm. With the testing wavelength $\lambda = 632.8$ nm, we obtain $d \leq 3.2$ m, so diffraction does not limit the measurement of a plate at Brewster's angle in the wide field mode. If $\Lambda = 1$ mm (in the narrow field mode), then $d \leq 20$ cm. A 10 cm square section of a plate at Brewster's angle has a range in depth of approximately 15 cm, so the edge of the RF that is nearest the tilted plate can be no farther than 5 cm from the plate. So, the full aperture of the tilted plate cannot be measured at $\Lambda = 1$ mm with a fixed set up, as one edge of the plate is at least 61 cm from the RF. The test piece (or the RF) must be repositioned so that the *minimum* gap between the RF and the 10 cm square test region of the tilted plate is less than 5 cm (Figure 4).

4. INTERFEROMETER LAYOUT

Figure 5 shows the basic layout of the interferometer. The system is a Fizeau design with several folds in the beam expansion path to reduce the footprint of the system to a compact 5 ft. wide x 6 ft. long envelope. A standard size 5 ft. x 12 ft. optical table allows sufficient test area for either brewster's angle or normal tests to be accomplished.

5. MECHANICAL DESIGN

The Mechanical design of all vibrationally sensitive elements in the interferometer was accomplished through extensive use of F.E.A. analysis. This allowed WYKO to accurately predict frequency response of critical elements, as well as ensure deformations were within tolerance limits.

5.1 Major mechanical elements

The major components are described below for the mechanical components of the system.

5.1.1 Phase shifter assembly

The phase shifter assembly as shown in figure 6 is an integrated assembly containing the PZT elements and the phase shift flexures, the transmission flat, cell, and adjusters, and the collimator and its mounting cell.

5.1.1.1 Transmission flat

The transmission flat cell is one of the most critical elements in the design. The cell must support and locate the flat to exceptional tolerances without significant deformation. Finite element analysis showed the rigid body modes of the transmission flat to be the most significant with respect to vibration response. This analysis also indicated that thin hard bonds with maximum edge contact area would best control the motion of the flat in the cell. Test scaled to 6 in. flats revealed that such bonds could not be reliably produced without significant deformation of the flat. By incorporating "Micro-G" connectors (patent pending) between the cell and the flat as shown schematically in figure 7, thick, low stress bond could be used and the connection between the cell and the flat would remain essentially rigid for the maximum accelerations expected. This provides reliable low deformation mounting of the flats and immunity to vibrational disturbances.

5.1.1.2 Phase shift flexures, tip-tilt adjusters, and PZTs

The phase shifter uses conventional piezoelectric actuators (PZTs) integrated into the system to push the flexures and ultimately the transmission flat to accomplish the phase shift. To minimize the mass, the PZTs must move. The interposing plate commonly used to mount the tip-tilt adjusters was eliminated. Figure 7 shows one of the three flexures used as well as one of two of the tip-tilt adjusters. The third flexure carries a spherical pivot bearing rather than the tip-tilt adjusters and is orthogonally arrayed around the flat. A unique feature of this design is a rigid coupling between the transmission flat cell and the phase shifter mechanism rather than the sprung connection commonly used. Also unique to this design, are the adjusters which are bolted to the flat cell and can be disconnected without decompressing any springs thereby reducing damage potential to the flat. The flat can be rotated in 90 degree intervals to allow for absolute testing. The resonance and response of the flexure assembly was also optimized using F.E.A. resulting in a system suitable for production environments. The software contains calibration algorithms to determine the correct amount of phase shift, the planarity and linearity of the phase shift.

5.1.1.3 Collimator

The collimator cell supports and locates the collimator as well as provides for a small degree of tip-tilt adjustment. The collimator must be aligned to the optical axis within 0.5 arc seconds to ensure proper control of emerging wavefront errors. The cell mounts directly to the phase shift support plate but incorporates no focus adjustment. Gross focus of the collimator is accomplished by translating the entire phase shift assembly. Fine focus is provided for in the adjustment of the laser source location.

5.1.2 Laser source assembly

The system requires the polarization of the laser be easily selectable between linear horizontal and linear vertical positions. The laser source assembly shown in figure 4 incorporates this feature in a novel way to eliminate alignment problems between the spatial filter and the laser during the lasers rotation. The laser source assembly, attenuation plates and spatial filter are a field replaceable unit. All rotate as a unit to change the output polarization state. The entire unit is replaced at laser service and requires no critical re-alignment by the user.

5.1.3 Imaging optics assembly

The system utilizes two magnifications: a wide field mode having a 43 x 43 cm. F.O.V. and a narrow field mode having a 10 x 10 cm. F.O.V.. The imaging system is toggled between the two settings via a remote hand held controller. A zero clearance crossed roller linear slide moves the optical sub-systems between hard stops to change F.O.V..

5.1.4 Camera panning system

In the high resolution mode the camera can be located at any point in the wide F.O.V. by the panning control. The position of the camera can be controlled via a joystick in the remote hand controller or by entering coordinates in the computer. Panning the camera removes the requirement of translating the test optic thus greatly simplifying the component mount, improving throughput, and decreasing damage potential to the test optic.

5.1.5 Alignment system

The interferometer employs three separate alignment systems. Two systems are used to provide coarse and fine alignment of the test piece resulting a large alignment field and easy fringe acquisition. The third system monitors the alignment of the return flat to better than $\lambda/2$. This ensures that the system will be easy to use and always within specification. The remote hand control is used to select alignment or test mode as well as coarse or fine alignment. When in test mode the alignment monitor displays a fringe pattern from a corner cube and the transmission flat. Keeping the flat aligned to within one fringe is adequate to meet specification.

5.1.6 Return flat

The Return flat is mounted similarly to the transmission flat above employing the same bonding method and "Micro-G" connectors. F.E.A. was also used to optimize the mount and ensure the bonding produced acceptably low levels of distortion. One major difference in the return flat is the truncated edges. To allow the return flat to be placed in close proximity to the transmission flat the edges were removed prior to final figuring. Figure 4 deals with the proximity requirement of the return flat. The flat is moved over the table using an integral air bearing. The flat must be positioned at different locations for different tests. A guide is provided to allow moving the flat along Brewster's angle for the narrow field measurements. This precludes any chance of contact between the flat and the test piece during setup.

5.1.7 Component mount

The component mount consists of two separate mounting fixtures. One for testing at Brewster's angle (without tip-tilt adjusters) and one for testing at normal incidence (with tip-tilt adjusters). The mounts are similar and are designed to receive frames into which the test optics have been previously mounted and allowed to thermally stabilize. The optics in general are large, heavy, delicate and extremely expensive. An overhead crane is required to handle the optical frames. Frames can be inserted into the mounts very quickly and easily facilitating throughput. The frame is lowered into a guide slot and aligned with a small spherical receiver in the mount. Frames carry forcing springs for the adjusters and are retained by gravity. The frames are interchangeable and reversible.

5.1.8 Optical table

The optical table was also subject to F.E.A. scrutiny. Two foot thick tables were specified to ensure that the cavity was not subject to vibration inducted by the bending mode of the table. The table is a standard size (5ft. wide 12 ft. long) keeping costs low. To keep the center of gravity within the stable pocket of the table the four isolation legs were recessed one foot and a third 3/16 in. thick stainless steel sheet was installed at this level to handle loads. Top and bottom are 3/16 in. stainless steel and the top is fitted with 1/4-20 threaded "clean holes" to facilitate mounting. The table acts as the base plate for the interferometer and the individual subassemblies and cover are bolted directly to it.

6. MAJOR OPTICAL ELEMENTS

The key components and the selected vendors are listed below for the first 24 in. interferometer.

6.1.1 Transmission flat

The transmission flat is being fabricated from Corning⁵ fused silica by the Eastman Kodak⁴. The flat is 25.5 in. diameter x 3.25 in. thick and is figured to $\lambda/10$ PV.

6.1.2 Return flat

The return flat is being fabricated from Corning⁵ ultra-low expansion (ULETM) fused silica by Kodak⁴. The flat is 25.5 in. diameter x 3.25 in. thick and has two parallel flat edges 17.4 in. wide. It is also figured to $\lambda/10$ PV.

6.1.3 Collimator

The collimator is an aspheric plano-convex singlet made from Schott³ BK7 glass by Kodak⁴. The element is 27 in. diameter by 2.92 in. thick. It has a maximum wavefront slope error of 0.5 arc seconds. Figure is 1λ P-V.

6.1.4 Folding mirrors

The folding mirrors range in size from 16 in diameter to less than 4 in. They are primarily Corning⁵ ultra-low expansion fused silica.

6.1.5 Imaging optics

The camera optics image the test piece directly onto the CCD. The narrow FOV optics are folded with mirrors into the same length as the wide FOV optics, so they can be switched using a simple linear slide. Focus and panning are performed by mounting the CCD camera onto a motorized XYZ stage.

7. PERFORMANCE OF PRE-PROTOTYPE

WYKO has manufactured a 24 in. phase shifting adapter previously for OCA⁶. Only the phase shifter assembly was designed or fabricated by WYKO with the customer providing the interferometer and optics from other sources. Figure 8 shows a histogram from a PZT calibration performed at OCA⁶. Because the mechanical stability of the OCA⁶ system is compromised in a number of ways (cantilevered table extensions, low performance mounts, etc.) vibration broadens the distribution by approximately a factor of two compared to all other WYKO instruments. While the OCA⁶ interferometer has performed adequately for its intended purpose (relatively low precision optical shop testing) we anticipate no difficulty in obtaining higher performance in the WYKO 24 in. system by employing superior mechanical and optical design.

8. SUMMARY

WYKO has designed a superior large aperture interferometer suitable for qualifying all N.I.F. large optics with exceptional resolution, and stability. Several unique features allow for rapid set ups and specialized testing methods. The system will allow quantification of the mid-spatial frequency errors most problematic to other, smaller systems as well as allow full use aperture testing on the large optics. The design is robust and intended for production environments. The system features a low noise high resolution detector (1000 x 1000 pixels), two fields of view (43 cm square and 10 cm square), Camera panning over full 43 cm aperture, remote controls, wide field alignment, and powerful Pentium® 32 bit PC computer control and data analysis.

9. ACKNOWLEDGMENTS

James Semrad performed the mechanical design and layout of the interferometer. Response Dynamics⁷ and ROM Engineering⁸ did the dynamic analysis of the system. Response Dynamics⁷ suggested the use of the "Micro-G" connectors.

This work was performed for the Lawrence Livermore National Laboratory under contract B324666.

Table 1. 24" Interferometer Measurement Characteristics

Mode	Parameter	Value
Wide Field	Field of View (\perp to beam)	43 \times 43 cm
	Pixel Pitch (\perp to beam)	0.44 \times 0.44 mm
	Largest Measurable Piece (At Brewster's Angle)	43 \times 78 cm
	Spatial Frequency (\perp to beam)	$\geq 0.25 \text{ mm}^{-1}$
Narrow Field	Field of View (\perp to beam)	10 \times 10 cm
	Field of Regard (\perp to beam)	61 cm diameter
	Pixel Pitch (\perp to beam)	0.10 \times 0.10 mm
	Spatial Frequency (\perp to beam)	$\geq 1.0 \text{ mm}^{-1}$
Both	Wavelength	632.8 nm

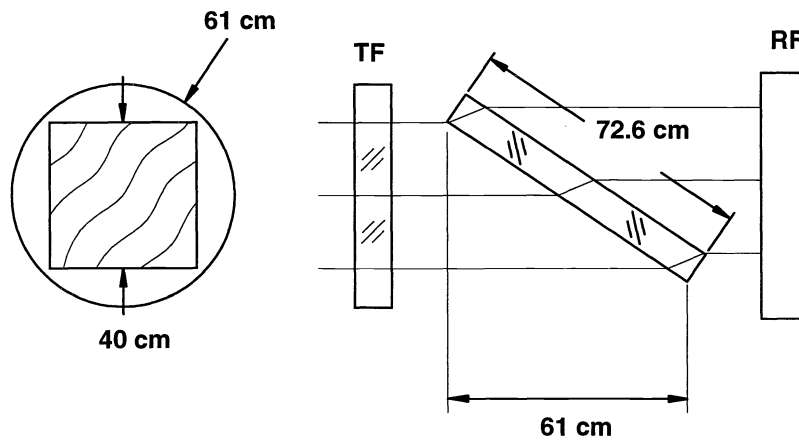


Figure 1. Testing a plate in transmission at Brewster's angle

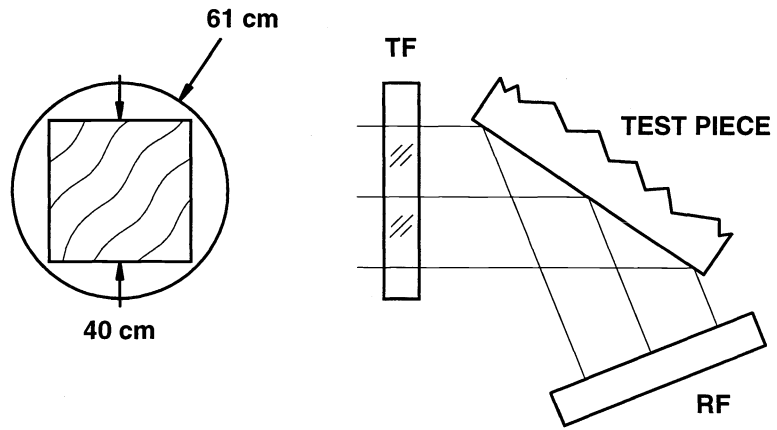


Figure 2. Testing a plate in reflection at Brewster's angle

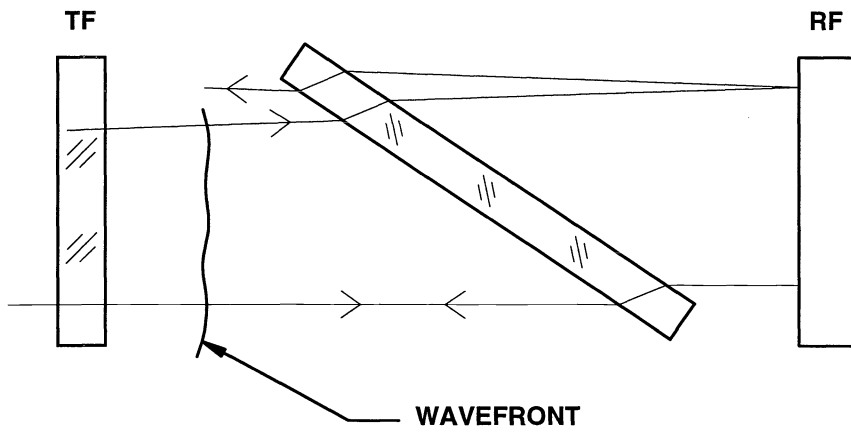


Figure 3. Beam walk-off

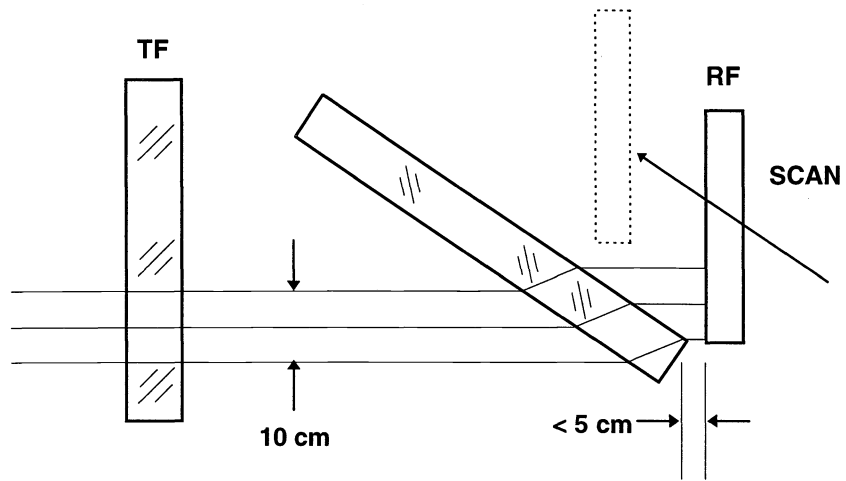


Figure 4. Movement of return flat for horizontal selection of subaperture

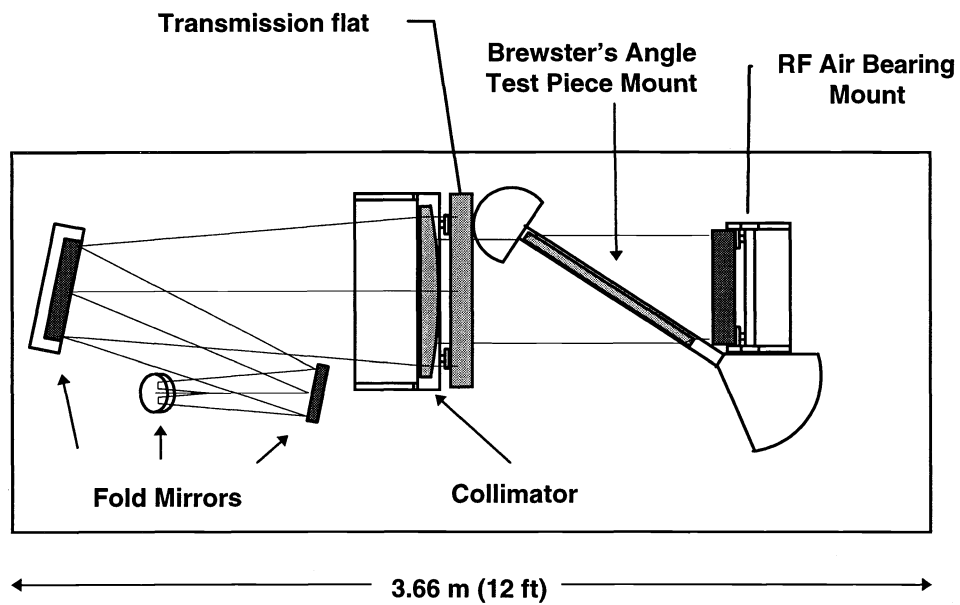


Figure 5. Plan view of interferometer on 5 ft. x 12 ft. optical table

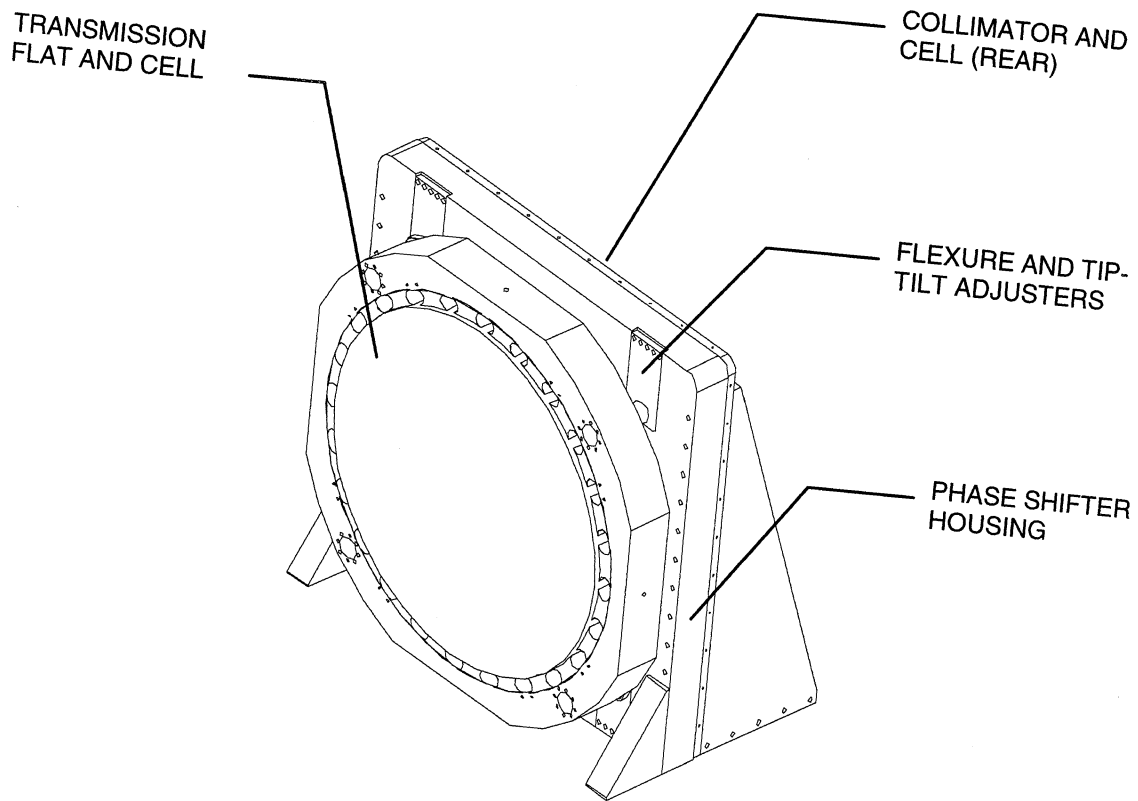


Figure 6 Phase Shifter Assembly

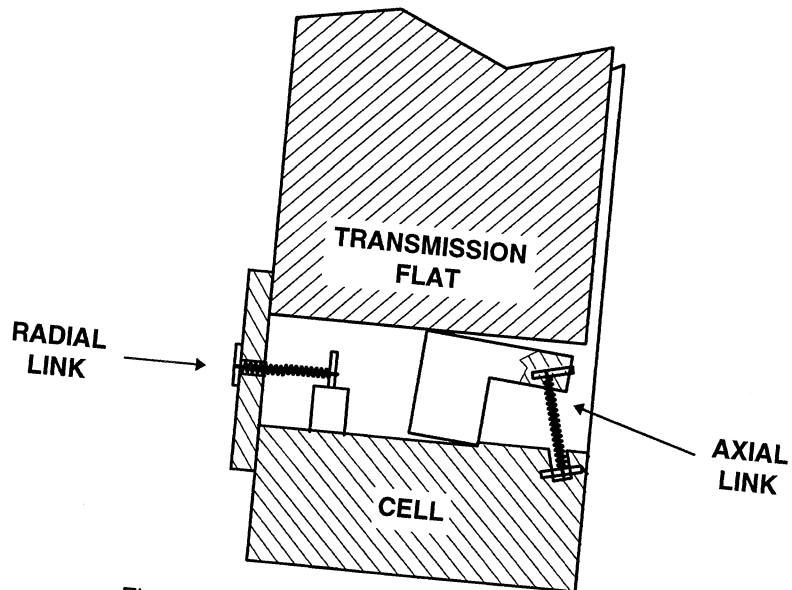


Figure 7 "Micro-G" connector (patent pending)

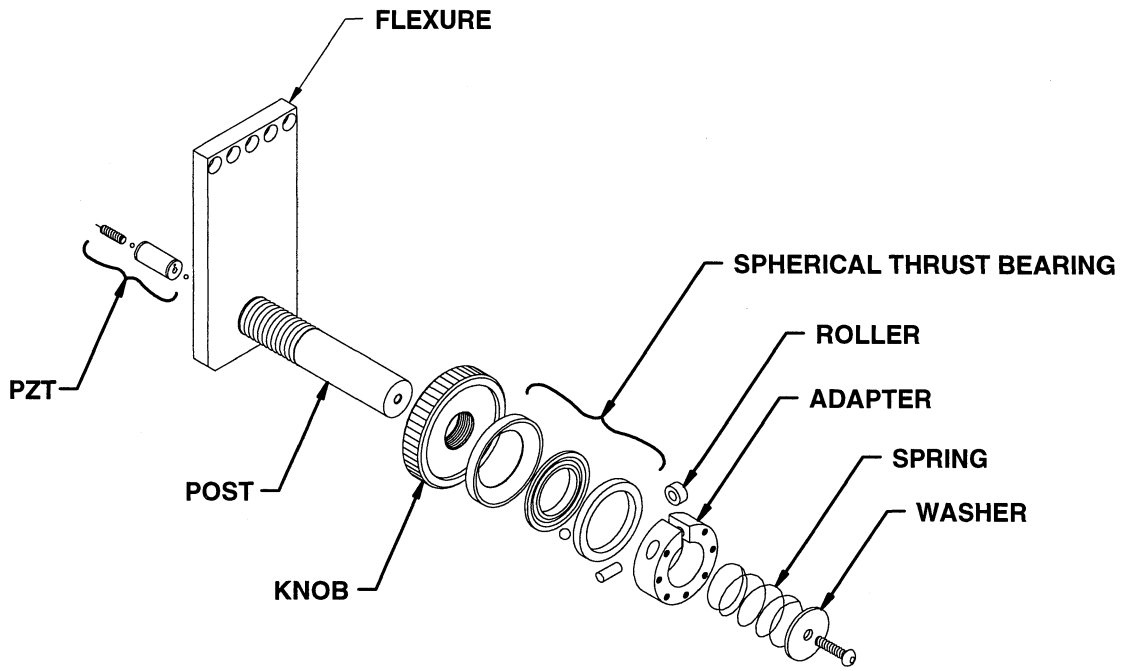


Figure 8 Flexure, with adjusters

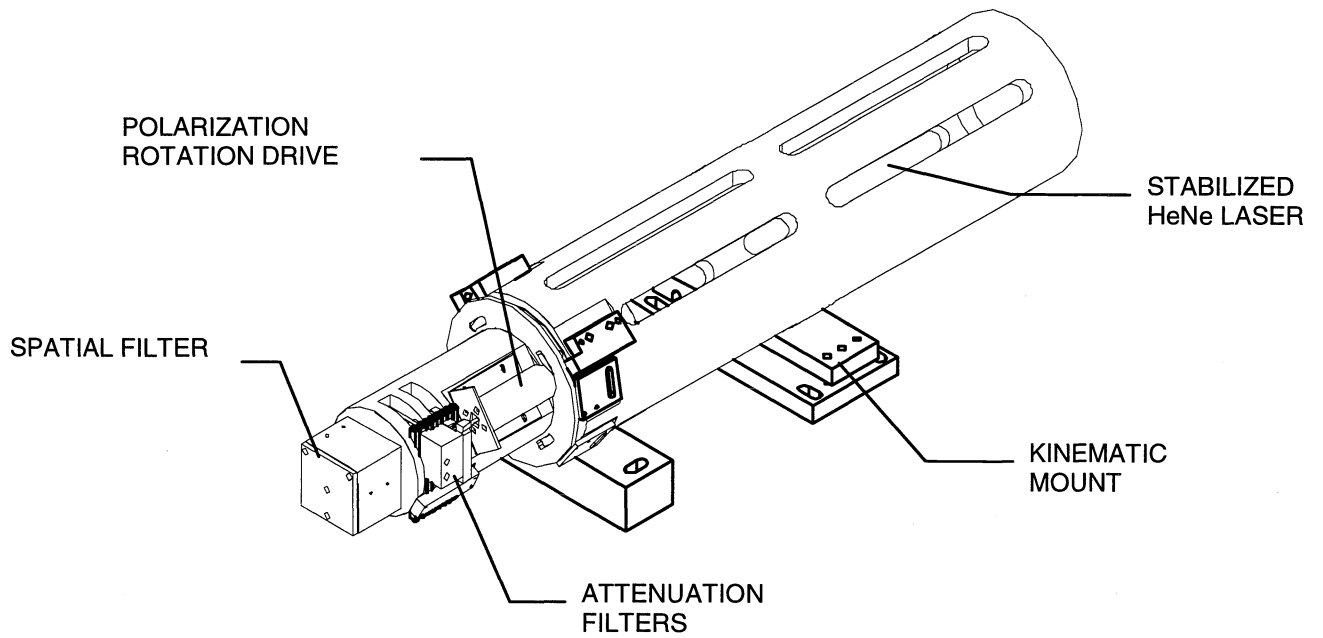


Figure 9 Laser source Assembly

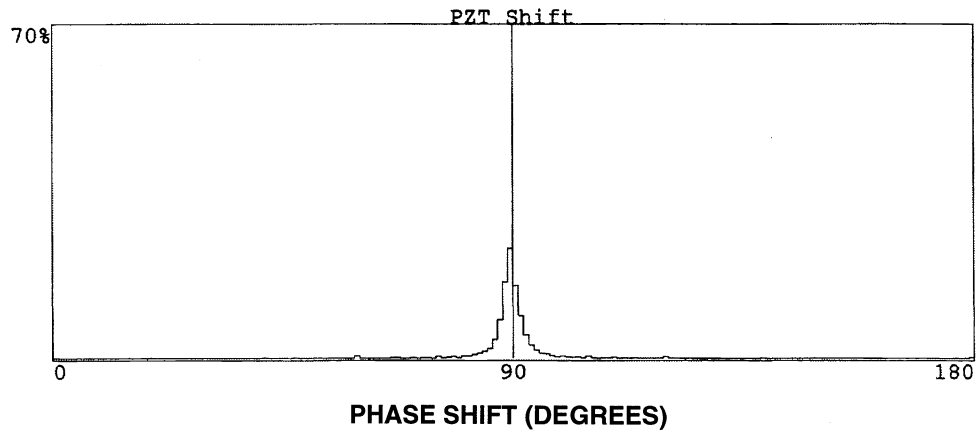


Figure 10. Calibration histogram for 24" phase shifter at OCA⁶

¹ Lawrence Livermore National Laboratory, P. O. Box 808, Livermore, CA, 94551-9900, USA

² J. W. Goodman, "Introduction to Fourier Optics", Second Edition, McGraw Hill, 1996

³ Schott Glass Technologies, Inc., 400 York Ave., Duryea, PA, 18642-2036, USA

⁴ Precision Optics, Commercial & Gov't Systems Div., Eastman Kodak Company, Building 601, Rochester, NY, 14650-3115, USA

⁵ Corning Inc., Advanced Products, 334 Country Route 16, Canton, NY, 13617, USA

⁶ Optical Corporation of America/OCA Applied Optics, 7421 Orangewood Ave., Garden Grove, CA, 92541, USA

⁷ Responce Dynamics, 5425 Masonic Ave., Oakland, CA, 94681, USA

⁸ ROM Engineering, P. O. Box 65170, Tucson, AZ, 85728